Naïve Bayes as a Probabilistic Tool for Monitoring the Health Status of Chronic Patients

Laura Teresa Martínez-Marquina[1][a], María Teresa Jurado-Camino[1][b],
Isabel Caballero-López-Fando[2][c] and Inmaculada Mora-Jiménez[1][d]

[1] *Dept. Signal Theory and Communications, Telematics and Computing Systems, Rey Juan Carlos University, Madrid, Spain*
[2] *University Hospital of Fuenlabrada, Madrid, Spain*

Keywords: Interpretability, Time-Dependent Patterns, Clinical Codes, Sex-Based Model, Clinical Decision Support.

Abstract: Chronic diseases have emerged as a pervasive global health concern, standing as a leading cause of mortality. Among these, prevalent conditions encompass diabetes, hypertension, congestive heart failure and chronic obstructive pulmonary disease. The large amount of data in Electronic Health Records is being exploited by machine learning schemes to design clinical decision support systems, usually of limited practical application because of lack of transparency. To overcome this issue and given the dynamic nature of the health-status over time, we propose here a patient health monitoring scheme based on a Näive Bayes approach because of its interpretability, minimal computational cost, and efficient handling of high-dimensional and unbalanced data. Our approach considers clinical codes (diagnosis and drugs) on real data collected by a Spanish hospital and provides a probability score for different chronic health-statuses. A gender-based approach has also been explored, exhibiting promising performance when there is a significant patient population for each sex. We conclude that pharmacological codes are more informative, although the best performance was obtained by using all the clinical codes and demographic features. Though a more exhaustive study on patient monitoring is necessary, the proposed NB scheme can be considered a proof of concept which has demonstrated to be a valuable tool and easily interpretable method.

1 INTRODUCTION

In recent years, there has been an alarming increase in the number of chronic patients, mainly in developed countries, due to the aging global population. Nearly 50% of the United States population (Raghupathi and Raghupathi, 2018) and 35% in Europe (Nolte et al., 2014), has some type of Chronic Condition (CC). CCs are the main cause of morbidity, being largely responsible for activity limitations in older adults and causing 60% of mortality (Atella et al., 2019). Furthermore, CCs entail significant socioeconomic repercussions that directly influence the healthcare system, amounting to 25% of the healthcare budget (Vandenberghe and Albrecht, 2020). This emphasizes the need for a paradigm change, drawing the attention not solely towards treating the illness, but rather towards its prevention (Vandenberghe and Albrecht, 2020) or slowing its progression. In this scenario, artificial intelligence and data-driven models can be of great assistance in achieving the well-known "Triple Aim" of healthcare systems, which is based on improving patient care experience, enhancing population health, and reducing medical care costs (Berwick et al., 2008).

In the healthcare context, Machine Learning (ML) is bringing about a true revolution, with increasing investment in research over the last decade. Automatically deriving insights from longitudinal Electronic Health Records (EHR) data offers new potential for clinical research, as patient information evolves through healthcare interactions (Zhao et al., 2017) across time. One of the main challenges of ML models on healthcare is their lack of interpretability. Ignoring this issue could greatly hinder the real-world utilization of data-driven models (Vellido, 2020).

Owing to the worsening effects of CCs, studying the temporal progression of chronic patients is vital. Given that their clinical journey is mirrored in diag-

[a] https://orcid.org/0009-0007-4975-1162
[b] https://orcid.org/0000-0002-5646-1290
[c] https://orcid.org/0000-0003-0193-4406
[d] https://orcid.org/0000-0003-0735-367X

Martínez-Marquina, L., Jurado-Camino, M., Caballero-López-Fando, I. and Mora-Jiménez, I.
Naïve Bayes as a Probabilistic Tool for Monitoring the Health Status of Chronic Patients.
DOI: 10.5220/0012353000003657

In *Proceedings of the 17th International Joint Conference on Biomedical Engineering Systems and Technologies (BIOSTEC 2024) - Volume 2*, pages 393-403
ISBN: 978-989-758-688-0; ISSN: 2184-4305

nosis and medication timelines, our paper suggests utilizing this data for health status monitoring and prediction. In the clinical setting, these predictions could be used by healthcare experts to establish intervention measures to slow down the progression of the CC. Specifically, in this paper we have considered demographic and clinical data of chronic patients associated with the University Hospital of Fuenlabrada (UHF) in Madrid region (Spain), with the research being previously approved by the Ethics Committee of the UHF. Our research group has already published some works in this topic, focusing on diabetic and hypertensive population (Soguero et al., 2020; Chushig-Muzo et al., 2022; Chushig-Muzo et al., 2020; Chushig-Muzo et al., 2021). In contrast to our previous articles, our focus in this paper expands the variety of CC and delves into the temporal monitoring of the chronic patient's health status. Specifically, we deal here with the following CC: diabetes, hypertension, congestive heart failure, and chronic obstructive pulmonary disease. Another distinction from our prior studies involves accounting for the sex variable. Though both genders demonstrate an escalating CC risk with age, this rise is often more dramatic among women (Ellis et al., 2022).

Thus, examining risk factors independently for men and women could substantially enhance the efficacy of tailored interventions for each gender.

As in our previous works, the identification of the chronic patients is carried out using the annual records of each patient and the Clinical Risk Group population grouper, since it is internationally validated (Hughes et al., 2004).

To characterize the patient's health status over time, we propose in this paper to use the Naïve Bayes (NB) scheme (Mitchell, 1997) due to its simplicity, efficiency in the handling of a large number of variables, complexity, transparency and interpretability, all of these very important items in clinical decision support systems. NB has been successfully applied within the medical domain (Al et al., 2012; Bhuvaneswari and Kalaiselvi, 2012; Hickey, 2013), encompassing a wide range of scenarios from estimating the risk of post-partum depression (Jiménez-Serrano et al., 2015) to, more recently, predicting the diagnosis of Alzheimer's disease (Chang et al., 2021). In this work, the NB approach has been used by considering both, continuous (age) and categorical variables (diagnosis and drug codes). As the NB classifier relies on the *Maximum A Posteriori* (MAP) decision rule (Demirbas, 1988), its probabilistic foundation enables identification of the most likely CC for a patient within a specific time frame, and also its associated probability. Note that the MAP rule takes into consideration the prior probability for every CC, so a careful analysis when dealing with highly unbalanced CC must be considered.

The rest of the paper is structured as follows. Section 2 presents our dataset description and corresponding exploratory analysis, focusing on the sex variable. The methods used for the temporal analysis and prediction of the patient's health status are in Section 3. Section 4 explains the process followed for the models' designs. The results obtained when evaluating different models, just considering demographic features, their combination with clinical codes, sex-based models, and the strategy for temporal monitoring are presented in Section 5. Conclusions are drawn in Section 6.

2 DATASET DESCRIPTION AND EXPLORATORY ANALYSIS

Demographic and clinical data were extracted from EHRs linked to the UHF, considering several types of chronic patients older than 18 years, getting a total of 16,791 patients (also named samples according to the ML terminology). Clinical data correspond to diagnostic and pharmacological records of these patients, both encoded using internationally recognized systems. Thus, diagnoses are coded according to the 9th revision of the International Classification of Diseases (ICD-9) and pharmaceuticals coded according to the Anatomical Therapeutic Chemical (ATC) classification system (Ronning, 2002).

The ICD-9 code consists of 5 Alpha-Numeric Characters (ANCs) with a decimal point between the third and fourth ANCs. Owing to the inclusion of new codes, this system has been renamed with the suffix CM (Clinical Modifications), ultimately referred to as ICD-9-CM (Association, 2004). The ATC code consists of 7 ANCs hierarchically structured into several levels: anatomical (first ANC, first letter of the anatomical group where the drug acts), therapeutic subgroup (second and third ANCs), pharmacological (fourth ANC), and chemical subgroup (fifth ANC). Although a quite complete definition of the pharmacological code is obtained with the first five ANCs, the chemical substance (sixth and seventh ANCs) provides additional information. To reduce data dimensionality (number of clinical codes) and in line with the methodology of previous studies in our group (Chushig-Muzo et al., 2022), we only consider here the first three digits of the ICD-9-CM and the five digits of the ATC codes, resulting in 1,517 diagnosis features and 746 drug features.

As in our previous works (Chushig-Muzo et al., 2022; Soguero et al., 2020; Chushig-Muzo et al., 2020; Chushig-Muzo et al., 2021), chronic patients were clinically identified according to a Population Classification System named Clinical Risk Groups (CRGs), internationally validated and oriented towards chronic patients (Hughes et al., 2004).

This system considers demographic factors (age and sex), clinical attributes (diagnoses, procedures, and medications), and the corresponding dates of patient encounters over a specified time frame, typically one year. Its purpose is to assign each patient to one of the 1,080 health statuses. The identification of the CRG health groups is denoted by a 5-digit code. The first digit represents the overall patient's health status, with 9 potential core health statutes: 1 (healthy), 2 (significant acute disease), 3 (single minor CC), 4 (minor CC in multiple organ systems), 5 (single dominant or moderate CC), 6 (significant CCs in multiple organ systems), 7 (dominant CC in 3 or more organ systems), 8 (dominant and metastatic malignancies) and 9 (catastrophic condition). The next three digits represent a more specific health condition and are referred to as base-CRG. The last digit is the severity level (not considered here).

As CRGs provide a clinically accepted categorization for identifying patients with significant CCs, they can be employed as the ground truth to guide a supervised ML task and construct a predictive model of the patient's health status. For this purpose, this study considers the more prevalent CCs: Congestive Heart Failure (CHF), Hypertension (HT), Diabetes (DIA) and Chronic Obstructive Pulmonary Disease (COPD). Since we will consider these CC and the combination of them, finally we will select only a total of 10 health status groups, from the 1,080 status groups available in the CRG system. Thus, patients with only one CC are assigned to CRGs where the first digit is 5, i.e, CRG-5179 (CHF), CRG-5192 (HT),and CRG-5424 (DIA). Note that COPD has not an specific CRG group. Individuals with two simultaneous CCs are assigned to CRGs starting with the number 6, i.e., CRG-6190 (CHF and COPD), CRG-6191 (CHF and DIA), and CRG-6313 (HT and DIA). Groups linked to more than two simultaneous CCs start with the number 7, i.e, CRG-7060 (CHF, DIA and COPD), CRG-7080 (CHF, DIA and other CC), CRG-7081 (CHF, COPD and other CC), and CRG-7140 (HT, DIA and other CC).

Considering all the previous aspects, the database comprised 16,791 patients with anonymous data records from the UHF, each uniquely identified with an ID and associated with just one of the aforementioned 10 CRG groups. For each patient, demographic data (age, sex) and clinical data (diagnoses, procedures, drugs) recorded during one year are available, along with the corresponding registration dates. All this information is used by the CRG system to assign every patient to one CRG group. Table 1 summarizes the demographic data per CRG.

Table 1: Statistics per CRG: number of patients, % of women and age (average, and standard deviation in brackets).

CRG	*# Patients*	*Women (in %)*	*Age*
5179	114	66.7	68.9(13.8)
5192	10,126	56.3	57.9(12.0)
5424	1,939	40.6	53.9(15.6)
6190	96	56.2	79.0(11.7)
6191	120	66.7	72.6(11.6)
6313	3,228	47.7	62.3(10.7)
7060	159	59.1	70.6(10.9)
7080	93	59.1	73.3(12.5)
7081	187	50.8	80.8(11.9)
7040	729	58.2	67.4(10.9)

Following our previous analysis (Chushig-Muzo et al., 2022; Soguero et al., 2020; Chushig-Muzo et al., 2020; Chushig-Muzo et al., 2021), every patient is characterized by a binary feature vector $\mathbf{x} = [x_1, x_2, \cdots, x_d, \cdots, x_D]$ with $x_d \in \{0,1\}$, composed by 1,517 diagnoses codes and 746 drug ones (D = 2,263 features). Each element of $\mathbf{x}$ is encoded with a value of '1' if the corresponding code was registered for the patient some time during the year, and with '0' otherwise. Thus, we can compute the presence rate for each code and CRG, creating the named "profile" for each CRG when considering all codes in a bar graph, as shown in other publications (Chushig-Muzo et al., 2021; Jurado-Camino et al., 2023) and not presented here for limitation space.

To gain knowledge of the most prevalent clinical code per sex linked to each CRG, an exploration of the profiles was carried out. The presence rate of the most common diagnosis and pharmacological codes on each CRG, separated by sex, is summarized in Tables 2 and 3, respectively. Note that the ICD-9-CM code with the highest presence rate in almost all the considered CRGs (excepting CRG-5424) is '401', representing Essential Hypertension (EHT). This is a result of the tight relation between HT and CHF (Pugliese et al., 2020), as well as of the association between insulin resistance and elevated blood pressure (Sowers, James R and Frohlich, Edward D, 2003). Other diagnosis codes with high rate are '428' (heart failure) and '250' (diabetes mellitus), which are commonly associated with all CRGs linked to cardiovascular and diabetic patients, respectively.

The highest presence rates in pharmacological codes are summarized in Table 3. The most prevalent medications start with the letters A, B, C, and N. In line with the anatomical classification previously presented, these letters represent the Alimentary, Blood, Cardiovascular, and Nervous systems, respectively. Although drugs beginning with A tend to be more associated with DIA and those beginning with C with cardiac problems, there are drugs commonly used across all CRGs as paracetamol or ibuprofen which primarily affect the Nervous system. These medications show some differences between women and men, which could be linked with period pains.

Table 2: Presence rate in each CRG when considering six of the most prevalent ICD-9-CM codes. Highest value for each CRG and sex (Men *M* and Women *W*) are in bold.

	IDC-9-CM Codes											
	250		***272***		***401***		***427***		***428***		***719***	
CRG	*M*	*W*	*M*	*W*	*M*	*W*	*M*	*W*	*M*	*W*	*M*	*W*
5179	0.03	0.05	0.29	0.16	0.40	0.42	0.50	0.39	**0.67**	**0.43**	0.14	0.14
5192	0.01	0.01	0.18	0.20	**0.70**	**0.68**	0.01	0.01	0.00	0.00	0.10	0.16
5424	**0.78**	**0.77**	0.17	0.17	0.06	0.07	0.00	0.00	0.00	0.00	0.10	0.12
6190	0.00	0.02	0.47	0.31	0.58	0.66	0.51	0.32	**0.79**	**0.76**	0.09	0.12
6191	**0.66**	**0.79**	0.24	0.32	0.32	0.63	0.31	0.44	0.48	0.52	0.15	0.17
6313	**0.78**	**0.76**	0.22	0.26	0.57	0.63	0.01	0.01	0.00	0.00	0.10	0.16
7060	**0.85**	0.77	0.42	0.42	0.54	0.58	0.51	0.45	0.66	**0.82**	0.13	0.12
7080	**0.86**	**0.84**	0.57	0.44	0.51	0.65	0.25	0.38	0.62	0.62	0.07	0.11
7081	0.16	0.26	0.23	0.44	0.42	0.59	0.58	0.56	**0.85**	**0.83**	0.03	0.10
7140	**0.75**	**0.72**	0.24	0.23	0.58	0.62	0.03	0.01	0.01	0.01	0.11	0.15

Table 3: Presence rate in each CRG when considering six of the most prevalent ATC codes. Highest value for each CRG and sex (Men *M* and Women *W*) are in bold.

	ATC Codes											
	A02BC		**A10BA**		**B01AA**		**C03CA**		**C10AA**		**N02BE**	
CRG	*M*	*W*	*M*	*W*	*M*	*W*	*M*	*W*	*M*	*W*	*M*	*W*
5179	0.69	0.67	0.00	0.00	0.64	0.67	**0.76**	**0.82**	0.60	0.46	0.52	0.72
5192	0.33	**0.47**	0.00	0.00	0.01	0.01	0.02	0.05	**0.33**	0.35	0.32	0.50
5424	0.27	0.41	**0.57**	**0.49**	0.00	0.01	0.01	0.02	0.49	0.44	0.29	0.44
6190	**0.97**	0.89	0.00	0.00	0.70	0.41	0.92	**0.95**	0.70	0.44	0.82	0.90
6191	0.74	0.88	0.65	0.38	0.61	0.61	**0.95**	**0.94**	0.66	0.72	0.62	0.76
6313	0.42	0.62	0.68	0.68	0.01	0.02	0.05	0.07	**0.68**	**0.69**	0.35	0.56
7060	0.91	0.91	0.39	0.37	0.43	0.62	**0.97**	**0.98**	0.64	0.62	0.80	0.91
7080	0.80	0.97	0.27	0.42	0.17	0.43	**1.00**	**0.95**	0.75	0.58	0.74	0.88
7081	0.96	0.97	0.08	0.10	0.40	0.50	**0.99**	**0.98**	0.38	0.47	0.94	0.96
7140	**0.65**	**0.75**	0.59	0.62	0.05	0.03	0.12	0.14	0.60	0.66	0.52	0.69

3 METHODS

We present here the fundamentals of the probabilistic approach used for prediction purposes, as well as the data preprocessing applied for subsequent temporal monitoring.

3.1 Naïve Bayes for Heterogeneous Data

Based on the Bayes' conditional probability theorem, the NB approach has shown good results under the naïve assumption that features are class independent (Mitchell, 1997). NB belongs to the family of MAP classifiers (Demirbas, 1988), which calculate the probability of the class conditioned to an specific feature vector. It stands out for its strong computational efficiency and ability to handle high-dimensional data effectively (Hickey, 2013; Al et al., 2012; Jiménez-Serrano et al., 2015; Bhuvaneswari and Kalaiselvi, 2012; Chang et al., 2021). NB can also use features of diverse nature (heterogeneous data).

As shown in Equation (1), given a set of C classes ($C = 10$ in this work) and vector $\mathbf{x}$, the NB scheme assigns to $\mathbf{x}$ the class maximizing the *posterior probability* $P(c_i|\mathbf{x})$.

$$\arg\max_{c_i} P(c_i|\mathbf{x}) = \arg\max_{c_i} \frac{P(\mathbf{x}|c_i)P(c_i)}{P(\mathbf{x})}, \qquad i = 1, \ldots, C \tag{1}$$

where $P(c_i)$ is the *prior probability* of class c_i, $P(\mathbf{x}|c_i)$ is the *likelihood* of class c_i and $P(\mathbf{x})$ is the *marginal probability*.

For the application of this NB framework, the nature of the considered variables must be taken into account. In the context of this study, heterogeneous data are used, considering both binary features (presence/absence of clinical and pharmacological codes, represented by features named as x_d and coded as '1'/'0', respectively) and the numerical feature "age" (represented by the feature named x_r). Thus, the D-dimensional binary vector $\mathbf{x}$ is transformed into a D+1-dimensional one named $\mathbf{x}$' when considering the "age" attribute too. As a result, according to NB, the likelihood of class c_i is estimated as:

$$\hat{P}(\mathbf{x}'|c_i) = \left[\prod_{d=1}^{D} \hat{P}(x_d = 1|c_i)^b (1 - \hat{P}(x_d = 1|c_i))^{1-b}\right] \hat{P}(x_r|c_i), i = 1, \cdots, C, \quad b \in \{0, 1\} \tag{2}$$

with the part within brackets representing the estimation of the likelihood of vector $\mathbf{x}$ following the Bernoulli distribution (Sinharay, 2010), and $\hat{P}(x_d = 1 |c_i)$ is estimated as the relative frequency of the d-th feature when it is "on" ($x_d = 1$). However, this may lead to a probability of 0 for feature values that are absent in the dataset, significantly affecting the estimation provided by Equation (2). To ensure non-zero likelihoods, a common practice is to apply Laplace smoothing (Kibriya et al., 2005).

Regarding the "age" variable, since the number of potential values is high (between 18 and 103 in this work), to use a frequentist approach with every possible value can lead to very abrupt changes in the probability between consecutive age values, especially in

CRGs with few patients. To address this issue, we proceed as if it were a continuous variable, obtaining the probability in intervals. In this work, the following six intervals were established for x_r on the basis of the exploratory analysis: ≤ 29; 30-40; 41-49; 50-59; 60-74; $\geq$75. Though the relative frequency could be used for estimating probabilities in each interval, we empirically found using synthetic data that more acute estimates were provided when getting the probability density function (*pdf*) in a non-parametric way by using Gaussian kernels and the Parzen windows method (Parzen, 1962; Silverman, 1986) and then integrating it to have the corresponding probability. Figure 1 shows both approaches for CRG-5179, CRG-6190 and CRG-7060, both for women and men.

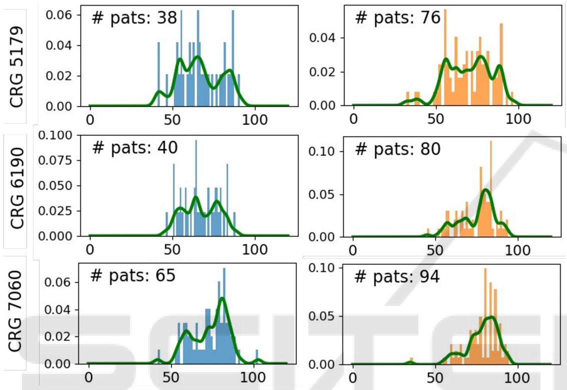

Figure 1: Normalized histograms for the age (left panels, blue, for men; right panels, orange, for women) and corresponding *pdf* estimation using Parzen windows (in green).

3.2 Data Preprocessing for Temporal Monitoring

In healthcare, time series are usually irregularly sampled, with irregular temporal intervals between two consecutive clinical registers. To address this issue,pharmacological data, reported on a monthly basis, are used in this work. However, the peculiarities of the Spanish health system, with a different EHR in each Spanish region (17 regions, with no interoperability between EHRs), can lead to data gaps in one of them over extended periods of time. These gaps may arise from factors like lengthy vacation periods, during which patients are away from their usual residence, resulting in no registration of the medication dispensation in their region. These gaps manifest as missing data in the patient's EHR accessible by the UHF.

In order to overcome the difficulties in the analysis produced by the lack of encounters with the regional health system, we carry out a preprocessing stage using temporal data.

In particular, we propose to use a exponential weighting function ensuring that the drug presence is not deactivated abruptly in the next month if the drug dispensation has not been registered. Instead, for each feature, exponential weighting functions are added and the result is used to create the new binary temporal values for the corresponding feature x_d after thresholding. Figure 2 shows an example of the temporal vector with twelve months, with the pharmacy symbol indicating that the drug has been collected (see the binary feature, with '1' value in Feb, Apr, May, Jul, Oct, Nov and Dec). Since the exponential function is continuous and we just have one value per month, the exponential weighting function of one month length (blue line in Fig. 2) is sampled every month. As displayed in Figure 2, when the sampled value is above the threshold (0.5, dotted red line), for each month the corresponding element is set to '1' ('0', otherwise) in the preprocessed feature. The new temporal sequence of values is shown in Fig. 2 as interpolated monthly feature. Note that, even when the drug is not dispensed on a monthly basis, the new values exhibit a scenario most similar to the ideal one (regular drug dispensation, linked to permanent use by chronic patients).

To deal with temporal data, it is common the use of sliding windows (Chen et al., 2017). In this work, the window length gather data over three months, encompassing also data from the preceding two months before the target month in which we want to predict the patient's health status.

4 EXPERIMENTAL DESIGN

We detail here the procedure to create the design and test sets, to overcome overfitting and achieve good generalization capabilities. Next, the model construction is explained.

4.1 Experimental Setup

For this study the dataset was split into design and test sets in a proportion of 70%-30%. The design set, used to train the NB model using feature vectors summarizing annual encounters, was further split into training (80%) and validation set (20%). The test set was used to evaluate the NB model considering two time scales: annual and quarterly. To avoid a bias linked to the use of a particular split, 10 different training-validation-test splits $\mathcal{X} = \{\mathcal{X}_1, ..., \mathcal{X}_{10}\}$ were performed.

Since feature vectors summarize the encounters over a relatively long period of time (annual or quar-

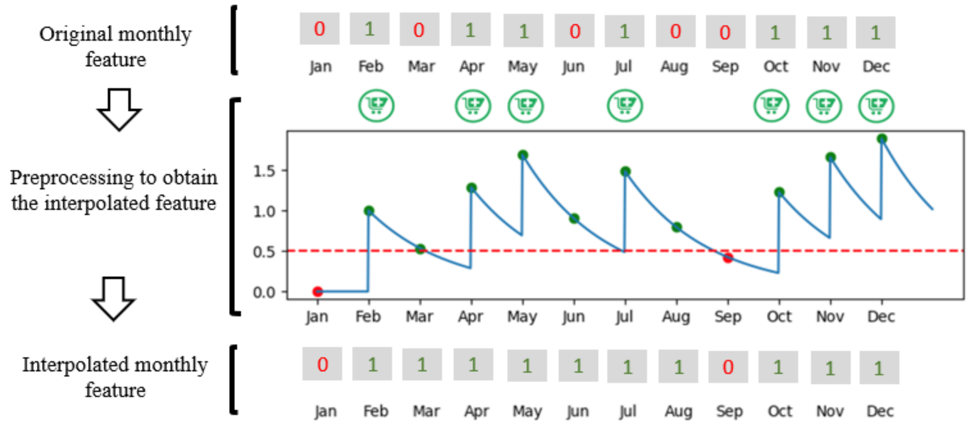

Figure 2: Top panel displays the original monthly feature vector for a specific drug, with '1' representing the drug dispensation with a pharmacy symbol in green. Middle panel shows the preprocessing applied to the original feature vector by using an exponential weighting function (in this case, with 1 month decay, see blue line). Bottom panel represents the preprocessed feature vector after thresholding the previous blue function with a 0.5 value (dashed red line).

terly), it is possible that different patients are represented by equal vectors.

Taking this into account, and with the intention of ensuring an appropriate design, it was checked that patients assigned to different CRGs were not represented by the same feature vector. Additionally, identical vectors associated with the same CRG (448 vectors in total) were temporarily removed from the dataset and grouped together in the set $\mathcal{R}$. Note that not all vectors in $\mathcal{R}$ are identical among themselves, but each one has at least another identical feature vector in $\mathcal{R}$. After the initial split of vectors not included in $\mathcal{R}$ into training, validation and test subsets, similar vectors in $\mathcal{R}$ were proportionally distributed in those subsets, as shown in Figure 3.

Regarding the sex-based models (separating women and men), a similar setup was carried out in parallel, resulting in 10 partitions for women $\mathcal{X}^{\mathcal{F}} = \{\mathcal{X}_1^F, ..., \mathcal{X}_{10}^F\}$ and another 10 for men $\mathcal{X}^{\mathcal{M}} = \{\mathcal{X}_1^M, ..., \mathcal{X}_{10}^M\}$.

4.2 Naïve Bayes Model Construction and Figures of Merit

Several NB models were explored by using the annual summary of clinical variables. First, two models using separately diagnoses codes and pharmacological codes were considered. Second, a model using both diagnosis and pharmacological (clinical) data, together with demographic data, was tackled. Finally, sex-based models were designed.

The NB performance was assessed using various figures of merit. Besides the accuracy rate for each CRG, we also considered the multiclass Confusion Matrix (CM) and the multiclass Receiver Operating Curves, with their corresponding Areas Under the Curve (AUC) (Hanley and McNeil, 1982). Together with the AUC per CRG, we also present the Macro-Average AUC and the Micro-Average AUC (weighted average based on the number of patients per CRG), usually used in multiclass tasks (Fodeh et al., 2021).

For each scenario (different input feature vectors), 10 models were designed (one model per partition in $\mathcal{X}$). In the case of sex-based models, partitions $\mathcal{X}^{\mathcal{M}}$ and $\mathcal{X}^{\mathcal{F}}$ were considered. For the NB hyperparameter selection, we explored four values of the Laplace smoothing parameter $\{0.01, 0.05, 0.1, 0.5\}$, being 0.05 or 0.1 the most selected values according to the the Macro-Average AUC on the validation set (see Figure 3).

5 RESULTS

This section presents the test results using a summary of the annual data and also considering sex-based models. The proof of concept with temporal monitoring throughout the year, conducted using pharmacological data, is finally presented.

5.1 Using Data Registered over a Year

Binary feature vectors summarizing the patient's clinical encounters during one year have been considered, designing two different models: the *Diagn-Model* uses only diagnoses features, while the *Pharm-Model* just considers pharmacological features. We explored both equiprobable schemes (yielding best outcomes)

Table 4: Average AUC per CRG (10 test partitions) when using different models, including sex-based ones (rightmost columns).

CRG	Diagn Model	Pharm Model	*Clinical&Demog Model*	*Clinical&Demog Men-model*	*Clinical&Demog Women-model*
5179	0.712	0.801	0.821	0.780	0.840
5192	0.864	0.893	0.952	0.955	0.953
5424	0.793	0.877	0.899	0.903	0.889
6190	0.640	0.711	0.697	0.610	0.636
6191	0.606	0.810	0.775	0.706	0.740
6313	0.729	0.811	0.857	0.869	0.862
7060	0.723	0.734	0.747	0.742	0.752
7080	0.603	0.660	0.636	0.590	0.623
7081	0.800	0.791	0.835	0.829	0.832
7140	0.752	0.725	0.787	0.759	0.803
Macro	0.722	0.782	0.801	0.774	0.793
Micro	0.817	0.862	0.912	0.913	0.914

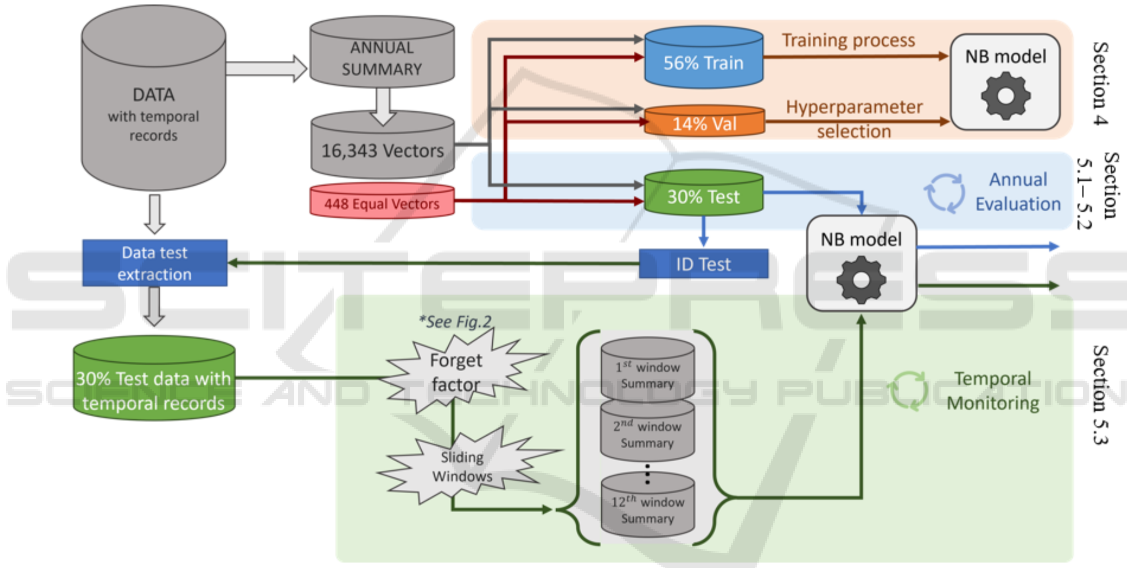

Figure 3: General framework for the NB model design, annual evaluation and temporal monitoring.

and a priori probability estimates based on the occurrence rate. The results presented in this paper correspond to equiprobable schemes.

When analyzing the test CMs with the annual summary data, we observed that the *Diagn-Model* shows more confusion between CRGs linked to one significant CD (CRGs starting with the number 5). The *Pharm-Model*, even using a lower number of features, improves the results linked to CRGs with dominant CDs in triplets (CRGs starting with the number 7), which is of paramount interest due to the worst health status of patients assigned to this kind of CRGs. These results show that drug codes are more informative than diagnosis ones.

Analizing the AUC values in Table 4, an improvement in macro and micro AUC is shown when comparing the *Pharm-Model* with the *Diagn-model*. We also observe best AUC values for the *Pharm-Model* in most of each particular CRG excepting those in the core health-status number 7 (more than two dominant CC). This lack of improvement could potentially be attributed to the lack of specificity in the third CC encompassed in this core health-status. Additionally, note that the annual summary may oversimplify the patient's characterization, making the task more difficult due to the complex patients' health status within these limited groups.

We also studied the performance when using all the clinical (diagnosis and pharmacological) codes and the demographic variable 'age'. As expected, the *Clinical&Demog-Model* provides the best values of Macro-Average AUC (0.801) and Micro-Average

AUC (0.912) and also the highest AUC for most of the CRGs. Among those showing no improvement (see Table 4), the CRG-6190 (CHF and COPD) is often erroneously associated with CRG-7081 according to the CMs in Figure 4. This confusion likely arises due to the shared CCs (CHF and COPD) and the lack of specificity in the third CC of CRG-7081 (CHF, COPD, and other CC). Additionally, observations suggest that when using the *Clinical&Demog-Model*, patients within CRG-6191 (CHF and DIA) display a higher level of confusion with those in CRG-6313 (HT and DIA). This could be attributed to the close relationship between CHF and HT, coupled with the limited specificity of the diagnosis code linked to EHT (401, one of the most prevalent codes across several CRGs, as shown in Table 2).

5.2 Sex-Based Analysis

The differences found in Section 2 when considering the "sex" variable suggested us to do a sex-based analysis when considering the best NB approach. Therefore, two models using both clinical and demographic features were created, designed and evaluated with patients of each sex separately.

Results in Table 4 show that for those CRG with a large or moderate number of patients (i.e. CRG-5192, CRG-6313, CRG-5424, with more than 1,000 patients) it is advantageous to design sex-based models. That is, the AUC provided by any of the sex-based (women and men) models with more than 1,000 patients is higher in comparison with the *Clinical&Demog-Model*. Apart from that, for CRGs with a low number of patients and also in comparison with the *Clinical&Demog-Model*, the best AUC is usually obtained with the sex-based model for which there is a higher prevalence in the CRG. Thus, this is the case of CRG-5179 (CHF), CRG-7060 (CHF, DIA and COPD) and CRG-7140 (HT, DIA and other) for the women-based model.

5.3 Temporal Monitoring

As previously mentioned in Subsection 3.2, for temporal monitoring it is desirable to work with a series regularly sampled. Owing to this reason, and also to the fact that our pharmacological data are automatically registered (they refer to dispensation since are also used for accounting purposes) and diagnoses are provided after codification of the clinical narrative, we decided to use the *Pharma-Model*.

Although chronic patients require a regular intake of specific medications, the medication records are not always consistently recorded on the EHR, and do not always accurately reflect patients' drug consumption. This can pose a challenge in the application of ML techniques, reason for introducing the "forget factor function" which gives exponentially less weight to the registration of ATC codes as time evolves. Different decay rates of the exponential weighting function were explored, allowing a certain presence of a particular ATC code to be maintained for more or less time. Decay values of zero, one, two, and three months were investigated. In general, as shown in Table 5, a slower decay of the exponential function led to better results in the accuracy rate for each CRG.

The only exception was CRG-5424 (DIA), in which the lower the decay value, the better the accuracy rate. In fact, the best result for this CRG was achieved with no decay value. This might be due to the different acute and occasional co-morbidities associated with diabetic patients, whose occasional treatment is more reflected in the patient's annual summary than in the quarterly one.

The accuracy rate obtained with the NB model trained when considering the presence/absence of ATC codes during one year are used as a baseline to evaluate the outcomes of the temporal monitoring (see first row in Table 5).

Regarding the quarterly results, the first value of each cell represents the average accuracy with results spanning from March to December, encompassing 10 values due to the exclusion of January and February (as these windows lack three months' worth of data). The second value, enclosed in parentheses, indicates the standard deviation of the accuracy rate. Note that the average accuracy rate for specific CRGs (5179, 5424, and 6191) within the quarterly scenario surpasses that achieved using annual summary data, particularly when employing a 3-month decay weighting function. Patients with a more severe health status, characterized by dominant CCs across three or more organ systems (indicated by gold-standard CRGs starting with 7), exhibit a higher accuracy rate with annual summary data compared to the quarterly approach. The limited 3-month data collection period might not adequately capture all the CC inherent to CRG7, potentially underestimating the patient's health condition into other CRGs sharing two of the CCs.

Continuing with the temporal monitoring, we focused on analyzing the posterior probabilities estimated by the model within each time window. These probabilities were examined from two distinct viewpoints: (i) First, the posterior probability $\hat{P}(\text{CRG}_i|\mathbf{x})$ was evaluated in cases where patients were associated with CRG$_i$; (ii) secondly, $\hat{P}(\text{CRG}_i|\mathbf{x})$ was assessed for patients not linked to CRG$_i$. In an optimal sce-

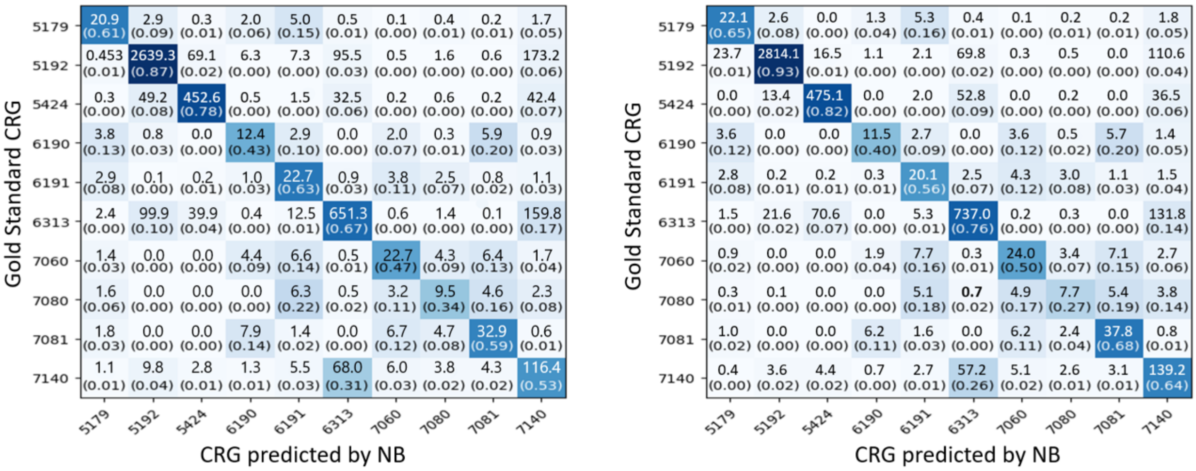

	5179	5192	5424	6190	6191	6313	7060	7080	7081	7140
5179	20.9 (0.61)	2.9 (0.09)	0.3 (0.01)	2.0 (0.06)	5.0 (0.15)	0.5 (0.01)	0.1 (0.00)	0.4 (0.01)	0.2 (0.01)	1.7 (0.05)
5192	0.453 (0.01)	2639.3 (0.87)	69.1 (0.02)	6.3 (0.00)	7.3 (0.00)	95.5 (0.03)	0.5 (0.00)	1.6 (0.00)	0.6 (0.00)	173.2 (0.06)
5424	0.3 (0.00)	49.2 (0.08)	452.6 (0.78)	0.5 (0.00)	1.5 (0.00)	32.5 (0.06)	0.2 (0.00)	0.6 (0.00)	0.2 (0.00)	42.4 (0.07)
6190	3.8 (0.13)	0.8 (0.03)	0.0 (0.00)	12.4 (0.43)	2.9 (0.10)	0.0 (0.00)	2.0 (0.07)	0.3 (0.01)	5.9 (0.20)	0.9 (0.03)
6191	2.9 (0.08)	0.1 (0.00)	0.2 (0.01)	1.0 (0.03)	22.7 (0.63)	0.9 (0.03)	3.8 (0.11)	2.5 (0.07)	0.8 (0.02)	1.1 (0.03)
6313	2.4 (0.00)	99.9 (0.10)	39.9 (0.04)	0.4 (0.00)	12.5 (0.01)	651.3 (0.67)	0.6 (0.00)	1.4 (0.00)	0.1 (0.00)	159.8 (0.17)
7060	1.4 (0.03)	0.0 (0.00)	0.0 (0.00)	4.4 (0.09)	6.6 (0.14)	0.5 (0.01)	22.7 (0.47)	4.3 (0.09)	6.4 (0.13)	1.7 (0.04)
7080	1.6 (0.06)	0.0 (0.00)	0.0 (0.00)	0.0 (0.00)	6.3 (0.22)	0.5 (0.02)	3.2 (0.11)	9.5 (0.34)	4.6 (0.16)	2.3 (0.08)
7081	1.8 (0.03)	0.0 (0.00)	0.0 (0.00)	7.9 (0.14)	1.4 (0.02)	0.0 (0.00)	6.7 (0.12)	4.7 (0.08)	32.9 (0.59)	0.6 (0.01)
7140	1.1 (0.01)	9.8 (0.04)	2.8 (0.01)	1.3 (0.01)	5.5 (0.03)	68.0 (0.31)	6.0 (0.03)	3.8 (0.02)	4.3 (0.02)	116.4 (0.53)

	5179	5192	5424	6190	6191	6313	7060	7080	7081	7140
5179	22.1 (0.65)	2.6 (0.08)	0.0 (0.00)	1.3 (0.04)	5.3 (0.16)	0.4 (0.01)	0.1 (0.00)	0.2 (0.01)	0.2 (0.01)	1.8 (0.05)
5192	23.7 (0.01)	2814.1 (0.93)	16.5 (0.01)	1.1 (0.00)	2.1 (0.00)	69.8 (0.02)	0.3 (0.00)	0.5 (0.00)	0.0 (0.00)	110.6 (0.04)
5424	0.0 (0.00)	13.4 (0.02)	475.1 (0.82)	0.0 (0.00)	2.0 (0.00)	52.8 (0.09)	0.0 (0.00)	0.2 (0.00)	0.0 (0.00)	36.5 (0.06)
6190	3.6 (0.12)	0.0 (0.00)	0.0 (0.00)	11.5 (0.40)	2.7 (0.09)	0.0 (0.00)	3.6 (0.12)	0.5 (0.02)	5.7 (0.20)	1.4 (0.05)
6191	2.8 (0.08)	0.2 (0.01)	0.2 (0.01)	0.3 (0.01)	20.1 (0.56)	2.5 (0.07)	4.3 (0.12)	3.0 (0.08)	1.1 (0.03)	1.5 (0.04)
6313	1.5 (0.00)	21.6 (0.02)	70.6 (0.07)	0.0 (0.00)	5.3 (0.01)	737.0 (0.76)	0.2 (0.00)	0.3 (0.00)	0.0 (0.00)	131.8 (0.14)
7060	0.9 (0.02)	0.0 (0.00)	0.0 (0.00)	1.9 (0.04)	7.7 (0.16)	0.3 (0.01)	24.0 (0.50)	3.4 (0.07)	7.1 (0.15)	2.7 (0.06)
7080	0.3 (0.01)	0.1 (0.00)	0.0 (0.00)	0.0 (0.00)	5.1 (0.18)	0.7 (0.02)	4.9 (0.17)	7.7 (0.27)	5.4 (0.19)	3.8 (0.14)
7081	1.0 (0.02)	0.0 (0.00)	0.0 (0.00)	6.2 (0.11)	1.6 (0.03)	0.0 (0.00)	6.2 (0.11)	2.4 (0.04)	37.8 (0.68)	0.8 (0.01)
7140	0.4 (0.00)	3.6 (0.02)	4.4 (0.02)	0.7 (0.00)	2.7 (0.01)	57.2 (0.26)	5.1 (0.02)	2.6 (0.01)	3.1 (0.01)	139.2 (0.64)

Figure 4: Average CM across the 10 test partitions for both the *Pharm-Model* (left) and the *Clinical&Demog-Model* (right). In each cell: the first value indicates the average count of test instances; the number within parentheses is the corresponding percentage, relative to the CRG established as the gold standard.

Table 5: Accuracy rate for each CRG using the summary over one year (Ann) and the average rate (and standard deviation, in brackets) when using the summary over quarterly sliding windows (Qua) with different weight decay.

CRG	***Ann***	***Qua*** ***0 m.***	***Qua*** ***1 m.***	***Qua*** ***2 m.***	***Qua*** ***3 m.***
5179	0.61	0.63 (0.02)	0.65 (0.02)	0.66 (0.01)	0.66 (0.01)
5192	0.87	0.76 (0.01)	0.77 (0.01)	0.78 (0.01)	0.77 (0.01)
5424	0.78	0.88 (0.01)	0.88 (0.01)	0.86 (0.01)	0.85 (0.01)
6190	0.43	0.27 (0.07)	0.33 (0.07)	0.39 (0.02)	0.42 (0.03)
6191	0.63	0.59 (0.02)	0.62 (0.02)	0.64 (0.03)	0.64 (0.03)
6313	0.67	0.60 (0.02)	0.60 (0.02)	0.60 (0.02)	0.60 (0.02)
7060	0.47	0.11 (0.04)	0.15 (0.04)	0.19 (0.04)	0.23 (0.03)
7080	0.34	0.21 (0.03)	0.24 (0.04)	0.28 (0.06)	0.28 (0.07)
7081	0.59	0.15 (0.03)	0.19 (0.03)	0.24 (0.03)	0.28 (0.04)
7040	0.53	0.34 (0.03)	0.38 (0.02)	0.42 (0.03)	0.44 (0.04)

nario, the probabilities in (i) should consistently be the highest among all those computed for the same vector **x**. However, this is not always the case, and at times, they may not rank as the highest probabilities. As illustrated in Figure 5 for CRG-5179, two box plots (green and red) were generated for each evaluation. The green boxes represent probabilities when the NB model correctly assigns the patient to the gold-standard CRG, while the red boxes depict instances where $\hat{P}(\text{CRG-5179}|\mathbf{x})$ isn't the highest (misclassified cases). This approach enables an evaluation of the "confidence" exhibited by the NB model when assigning patients to CRG-5179 (in this representation), while facilitating a comparison of outcomes obtained from annual and quarterly summary data. Note that, when considering cases assigned to CRG-5179, the median of the posterior probabilities (green) consistently remains above 0.8, particularly from the month of March onward.

Concerning $\hat{P}(\text{CRG}_i|\mathbf{x})$ for patients not associated with CRG$_i$, the focus is on identifying cases where this probability holds the highest value, leading to an incorrect assignment to CRG$_i$. In Figure 6, the gold standard CRG is presented in the vertical axis (9 box plots among the 10 CRGs) and probabilities of the misclassified samples are organized according to the actual CRG they are linked to, both for the annual summary data (left panel) and two representative situations of the quarterly summary data (two panels on the right). In this context, a significant increase is observed in the number of patients misclassified as CRG-5179, particularly among those originally linked to CRG-5192, CRG-5424, and CRG-7140, when quarterly summary data is employed. However, the probability distribution corresponding to these misclassifications remains similar to those estimated using annual data.

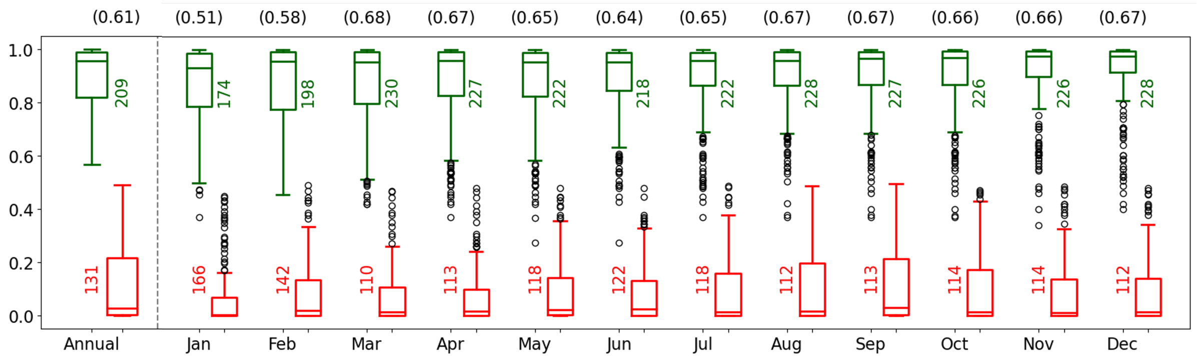

Figure 5: Count of test patients and statistics of $\hat{P}(\text{CRG}-5179|\mathbf{x})$ for the NB scheme when patients linked to CRG-5179: annual data summary (leftmost panel) and quarterly data summary (3 months) for each month. Green/red, for correctly/wrongly labelled patients. Accuracy rates are in brackets at the top.

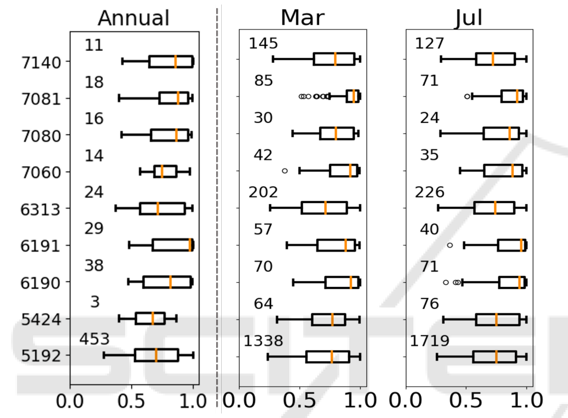

Figure 6: Count of test patients and box plots of $\hat{P}(\text{GRG}-5179|\mathbf{x})$ when it emerges as the highest value, despite the gold-standard CRG is in the vertical axis. Annual data (left panel) and quarterly data summary linked to windows centered on March and July (panels right of the dotted line).

6 CONCLUSIONS AND FUTURE WORK

Despite the straightforward nature of the Naïve Bayes approach, its application as a tool for identifying and monitoring patient health statuses has yielded promising outcomes, particularly when incorporating clinical codes and demographic attributes. Notably, in scenarios with a substantial sample size (such as CRG-5192, 5424, and 6313), an approach based on gender has exhibited advantages. This avenue opens the opportunity to investigate how gender influences the health conditions of chronic patients. Furthermore, the adoption of a gender-based feature selection strategy could potentially address the issue of high dimensionality, thereby positively impacting the model's performance.

Healthcare monitoring involves real data exhibiting a sequential structure, thereby implying that the interpretation of a pattern can be influenced by contextual information. To take temporal dependencies into account, we are currently exploring the use of recurrent neuronal models and its application to streaming data, seeking to enhance our monitoring capabilities.

In scenarios involving chronic patients, it would be also interesting to consider the incorporation of additional rules within the monitoring framework to enhance performance. This may be particularly pertinent given that the intrinsic nature of CCs indicates that the patient's health status (in the context discussed in this study, denoting CRG assignment) cannot experience improvement.

ACKNOWLEDGMENT

This work was partly funded by the Spanish Research Agency, grant number PID2019-106623RB-C41/AEI/10.13039/501100011033 (BigTheory), PID2022-136887NB-I00 (POLIGRAPH) and by the European Union NextGeneration-EU funds (Youth Employment Plan of the Spanish Government) in the INVESTIGO project with reference URJC-AI-11.

REFERENCES

Al, K. et al. (2012). Medical data classification with naive bayes approach. *Information Technology Journal*, 11(9):1166–1174.

Association, A. M. (2004). *ICD-9-CM 2005: International Classification of Diseases, 9th Revision Clinical Modification (Physician Edition)*. American Medical Association Press.

Atella, V. et al. (2019). Trends in age-related disease burden and healthcare utilization. *Aging Cell*, 18(1):e12861.

Berwick, D. M., Nolan, T. W., and Whittington, J. (2008). The triple aim: care, health, and cost. *Health Affairs*, 27(3):759–769.

Bhuvaneswari, R. and Kalaiselvi, K. (2012). Naive bayesian classification approach in healthcare applications. *International Journal of Computer Science and Telecommunications*, 3(1):106–112.

Chang, C.-H., Lin, C.-H., and Lane, H.-Y. (2021). Machine learning and novel biomarkers for the diagnosis of alzheimer's disease. *Intl. J. Mol. Sci.*, 22(5):2761.

Chen, M. et al. (2017). Disease prediction by machine learning over big data from healthcare communities. *IEEE Access*, 5:8869–79.

Chushig-Muzo, D., Soguero-Ruiz, C., de Miguel, P., and Mora-Jiménez, I. (2021). Interpreting clinical latent representations using autoencoders and probabilistic models. *Artif Intellig in Medicine*, 122:102211.

Chushig-Muzo, D., Soguero-Ruiz, C., de Miguel, P., and Mora-Jiménez, I. (2022). Learning and visualizing chronic latent representations using electronic health records. *BioData Mining*, 15(1):1–27.

Chushig-Muzo, D., Soguero-Ruiz, C., Engelbrecht, A., de Miguel, P., and Mora-Jiménez, I. (2020). Data-driven visual characterization of patient health-status using electronic health records and self-organizing maps. *IEEE Access*, 8:137019–31.

Demirbas, K. (1988). Maximum a posteriori approach to object recognition with distributed sensors. *IEEE Transactions on Aerospace and Electronic Systems*, 24(3):309–313.

Ellis, R. et al. (2022). Development and assessment of a new framework for disease surveillance, prediction, and risk adjustment:the diagnostic items classification system. In *J Am Med Ass Health Forum*, volume 3.

Fodeh, S. J. et al. (2021). Utilizing a multi-class classification approach to detect therapeutic and recreational misuse of opioids on twitter. *Computers in Biology and Medicine*, 129:104132.

Hanley, J. A. and McNeil, B. J. (1982). The meaning and use of the area under a Receiver Operating Characteristic curve. *Radiology*, 143(1):29–36.

Hickey, S. J. (2013). Naive bayes classification of public health data with greedy feature selection. *Communications of the Institute of Mathematics and its Applications*, 13(2):7.

Hughes, J. S., Averill, R. F., et al. (2004). Clinical risk groups (crgs): a classification system for risk-adjusted capitation-based payment and health care management. *Medical Care*, pages 81–90.

Jiménez-Serrano, S. et al. (2015). A mobile health application to predict postpartum depression based on machine learning. *Telemedicine and e-Health*, 21(7):567–574.

Jurado-Camino, M., Chushig, D., Soguero, C., de Miguel, P., and Mora, I. (2023). On the use of generative adversarial networks to predict health status among chronic patients. In *Health Informatics*, pages 167–178.

Kibriya, A. M. et al. (2005). Multinomial naive bayes for text categorization revisited. In *Austr J Conf on Artificial Intelligence*, pages 488–99.

Mitchell, T. M. (1997). *Machine Learning*. McGraw Hill.

Nolte, E. et al. (2014). Assessing chronic disease management in european health systems. concepts and approaches. *World Health Organiz.*

Parzen, E. (1962). On estimation of a probability density function and model. *The Annals of Mathematical Statistics*, 33(3):1065–76.

Pugliese, N. R. et al. (2020). The renin-angiotensin-aldosterone system: a crossroad from arterial hypertension to heart failure. *Heart Failure Reviews*, 25:31–42.

Raghupathi, W. and Raghupathi, V. (2018). An empirical study of chronic diseases in the united states: a visual analytics approach to public health. *Intl J. of Env. Research and Public Health*, 15(3):431.

Ronning, M. (2002). A historical overview of the atc/ddd methodology. *World Health Organization drug information*, 16(3):233.

Silverman, B. W. (1986). *Density Estimation for Statistics and Data Analysis*. London: Chapman & Hall.

Sinharay, S. (2010). *International Encyclopedia of Education*, chapter Discrete probability distributions. Elsevier Science.

Soguero, C., Mora, I., Mohedano, M. A., Rubio, M., de Miguel, P., and Sanchez, A. (2020). Visually guided classification trees for analyzing chronic patients. *BioMed Central Bioinformatics*, 21:1–19.

Sowers, James R and Frohlich, Edward D (2003). Insulin and insulin resistance: impact on blood pressure and cardiovascular disease. *The Medical clinics of North America*, 87(5):s1005–s1027.

Vandenberghe, D. and Albrecht, J. (2020). The financial burden of non-communicable diseases in the european union: a systematic review. *European Journal of Public Health*, 30(4):833–839.

Vellido, A. (2020). The importance of interpretability and visualization in machine learning for applications in medicine and health care. *Neural Computing and Applications*, 32(24):18069–18083.

Zhao, J. et al. (2017). Learning from heterogeneous temporal data in electronic health records. *J. Biomedical Informatics*, 65:105–119.